MINERAL EXPLORATION BY USING HYPERSPECTRAL IMAGE CLASSIFICATION AND "DOMING" DELINEATION [1]

Erzsébet Merényi
University of Arizona, Lunar and Planetary Laboratory
Tucson, AZ 85721, erzsebet@pirl.lpl.arizona.edu

Valentina Sumin–Finn
University of Arizona, Department of Geosciences
Tucson, Arizona 85721

Brian S. Penn
Pan–American Center for Earth and Environmental Studies
University of Texas at El Paso, Department of Geology
El Paso, TX 79968

ABSTRACT

We present work in progress, involving a new interdisciplinary approach that offers promise for mineral exploration. Two fully independent data analyses are combined. "Doming" delineation, which predicts the locations of endogenetic mineralization from topographic features. This procedure relates the surface expression of mineralization to endogenetic processes that lead to mineralization. It has long been successfully applied to mineral exploration by former Soviet scientists. Classification of high spectral resolution Visible and Near-Infrared signatures from a hyperspectral AVIRIS image of the same area identifies locations that show alterations involving iron oxides, oxyhydroxides, clays such as kaolinite and sericite, and other possible ore indicators. The combined results yield higher confidence in the prediction of mineralization than would either method alone. The Manhattan Mining District, Nevada, is used to illustrate the procedure.

1.0 BACKGROUND

The Manhattan Mining District (Figure 1) has been one of the major gold producers in Northern Nye County, Nevada. Numerous mines and prospects, old and new, extend well beyond the district proper. Mining was continuous from 1905 to 1947 with some activity in the late 1970's continuing to this time. Gold was the main commodity, with some production of silver, antimony and arsenic ores. Mercury, tungsten and nickel deposits received minor exploration. An extensive older literature describes the geological and mining information of Manhattan (*e.g.,* Ferguson, 1924; Kleinhampl and Ziony, 1984, p.140–149; and many others). The geological record of the southern Toquima Range, where the Manhattan District is located, indicates at least six major episodes of tectonism, volcanism, and plutonism during the Tertiary. Paleozoic metamorphic sedimentary rocks of Cambrian, Ordovician, Permian and Triassic ages comprise a total estimated thickness of 3350 m. These include a Paleozoic serpentinite–greenstone assemblage of about 150 – 350 m. The Cambrian Gold Hill Formation consists mainly of phyllitic to schistose and quarzitic strata and minor marble beds. The major ore deposits are commonly confined to specific units, such as the

[1] In Proc. Thirteenth International Conference on Applied Geologic Remote Sensing. Vancouver, British Columbia, Canada, 1–3 March 1999. Vol. I, pp 308–315.

White Caps, Carrera, Gold Hill formations of limestone and schist of Cambrian and Ordovician. Permian rocks lie unconformably on or are faulted onto the Lower Paleozoic rocks. It is inferred that many thousands of feet of intervening Middle Paleozoic strata were removed by erosion. Also the Lower Paleozoic strata may have been refolded when the Permian was deformed during a Post–Permian event, permitting Permian rocks in the cores of synclinal folds to be preserved from later erosion.

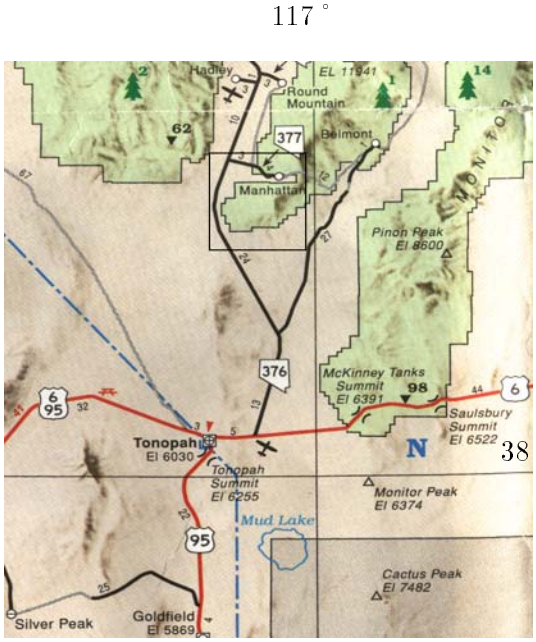

Figure 1. The location of the Manhattan mining district, Nevada. The black box indicates the area of the Manhattan dome structure, which is shown in Figure 2.

The Nevadan Orogeny is considered to have been concluded by the end of the Early Cretaceous, when mild doming processes accompanied the intrusion of granitic plutons aligned along the major fold trend of one of the earlier deformations. The doming process relates to the intrusion of aplitic and pegmatitic magmas about 80 m.y. ago. Another erosion interval followed and was superseded by intense volcanism in the Tertiary, associated with possible caldera formation and limited continental sedimentation, exposed north of the Manhattan mines. Basin–and–range faulting affected the Tertiary rocks and continued episodically into the Quaternary. The Late Cretaceous intrusive body of granitic rocks developed a marginal zone of feldspar phenocrysts, aplitic and pegmatitic dikes and is believed to be a cupola of the same stock in contact. It deformed the Cambrian and Ordovician strata, indicating mild doming during intrusion. A small body of diorite could be Tertiary, including the diorite near Round Mountain. Gabbro north of the mouth of Manhattan Gulch could be related to the serpentinite–greenstone unit. Some units in the main pile of Tertiary volcanic rocks north of Manhattan are genetically related to an hypothesized collapsed caldera–bounding fault that may have been intruded by Maris Rhyolite. Pliocene to Holocene gravels in several stages of erosion are preserved in Manhattan Gulch where placer mining was done. Ferguson (1924) described the gravels as minor remnants of Late Pliocene gravel probably formed on Late Pliocene postmature topography prior to or during the earliest development of Manhattan Gulch. Pleistocene gravels, now commonly covered by Holocene alluvium, are preserved on low terraces and at the base of the gulch. Pleistocene vertebrate fragments were recovered from an older, bouldery, clay–cemented gravel that rests on bedrock.

2.0 DATA AND ANALYSES

2.1 DOME DELINEATION

Many of the most valuable mineral districts display structural controls associated with endogenetic doming processes. The latter comprise multi–scaled latent concentric structures as domes, calderas, and deep linear trends. It is understood that the control of mineral districts and ore deposits comes about through complex interactions of convective, thermodynamic and geochemical processes. Migration and concentration of valuable minerals occur in structural “channels”

organized within the whole morphostructure. The domes are usually of latent character, being covered by sedimentary, magmatic, or volcanic rocks. Various surface phenomena can be interpreted to reflect the influences of subsurface tectono–magmatic activity through all overlying strata. Morphostructural analysis integrates the effects of long–lived endogenetic processes and tectonic movements. It determines relationships among surface and internal hidden dislocations that are expressed through their subtle influence on overlying crustal and sedimentary rocks. This results in an inherited character of tectono–magmatic activity through geological time. Morphostructural analysis was previously described by Baker (1993) and by Sumin–Finn *et al.,* (1995).

The conventional geological interpretation holds that this region is a part of a Tertiary type post–platform volcano–magmatic zone that developed on a basement of heterogeneous Paleozoic structures. The region corresponds to the SW part of the Nevada's Ridge–and–Valley tectonic province. The present relief began to develop during the Neogene with the formation of relief macroforms such as uplifts, mountain belts, depressions, and major drainage lines. Later uplift led to dissection and dismembering of relief, which formed deep valleys and high mountains. Various planation surfaces occur between elevations of 5,000–11,000 feet. Conditions here were especially favorable for the preservation of relict pre–Neogene planation surfaces. For this region morphostructural analysis was applied at scales of 1:250.000, 1:100.000, and 1:24 000. It revealed an autonomous oval dome structure of about 15 km in diameter in the southern part of the Toquima Range (Figure 2). This dome comprises an assemblage of smaller domes from 3 to 1 km in size, with radial and concentric dislocations (ridges and depressions). Blocks and sectors show the typical hierarchical pattern consisting of the concentric distribution of smaller domes inside larger ones. Endogenetic activities produced this interpreted pattern. The southeastern part of the 15 km Manhattan dome sank in displacements of different blocks, and the northern part of the dome is cut by a wide NWW linear trend of dislocations. The dome also exposes NW, NE, and NS trends of dislocations.

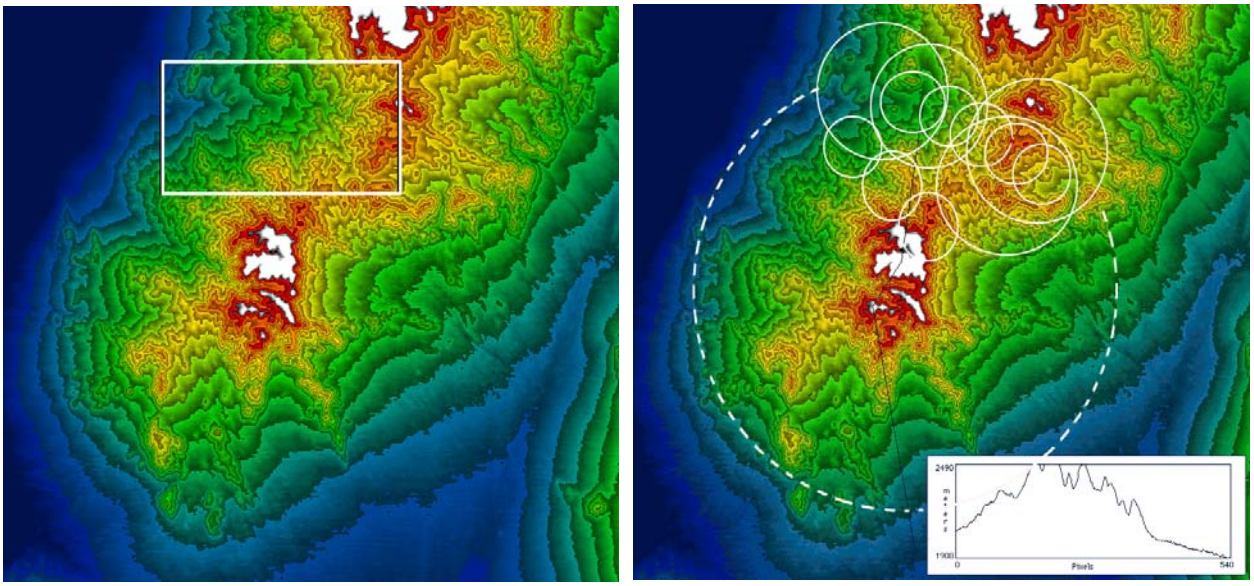

Figure 2. Left: The large–scale topographic form of the Manhattan mineral district, Nevada, derived from 7.5 minute DEMs. The white box indicates our study area. Right: The large–scale dome structures of the Manhattan area as determined by morphostructural analysis. The main dome, $\sim$ 15 km across, has a central, elevated block surrounded by a second range of smaller domes about 3 km in diameter. Only the smaller domes of the study area are indicated. Along with radial horsts, valleys, and blocks revealed on the surface, these all comprise a concentric hierarchical pattern of mineragenetic dome and caldera structures.

To derive the locations of possible structurally controlled mineralization, 7.5 minute USGS Digital Elevation Maps and 1:24,000 USGS topographic contour maps were used. Morphostructural interpretation at local scales can suggest the most promising sites to about 100 x 100 m^2 for further detailed checking. Interpretation and synthesis of geological and other available data such as spectral images, in relation to the morphostructural maps will predict the best areas for detailed exploration before costly drilling and detailed field work.

Figure 3 is a 1:24,000 topographic map of part of the Manhattan mining area, corresponding to the box in Figure 2. Further details of the circular dome structures are expanded here with respect to Figure 2. Areas of possible mineralization are predicted within the circular structures outlined by morphostructural analysis. The most probable locations of mineralization and ore deposits are indicated by small circles. Known mines in production are indicated by black dots.

The northern part of the Manhattan Dome is affected by NWW linear fracture dislocations in an irregular zig-zag-like trend. The chain of superimposed smaller circular structures 5 km to 1 km is nestled along of this weakness zone (Figure 3). These domes reflect the interaction between rising magma chambers and the surface. The heat, pressure, gases of intrusive Tertiary volcanic activity led to processes of extraction, migration, alteration and accumulation of valuable minerals in the upper levels of the crust. Experience with prognostic metallogenic analysis of distribution of mineralization shows the most promising zones for exploration will likely occur at the intersections of these smaller domes with linear hidden dislocations along the NNW trend.

2.2 HYPERSPECTRAL VIS–NIR IMAGE ANALYSIS

A hyperspectral Visible and Near Infrared (VIS–NIR) AVIRIS image was used for the identification of surface spectral properties. Acquired on June 18, 1998, it covers approximately 10 x 12 km^2 centered over the flight line (38.50 $^\circ$N, 117.15 $^\circ$W) to (38.50 $^\circ$N, 117.05 $^\circ$W). The spatial resolution is approximately 20 m/pixel, and the spectral resolution is 10 nm, which is sufficient to resolve fine narrow features such as specific clay bands. The spectral window, 0.38–2.5 μm, includes wavelengths where characteristic manifestations of iron oxides, oxyhydroxides, clays and other alteration products occur.

Preprocessing included atmospheric correction using ATREM 3.0 (Gao *et al.,* 1997), and normalization of the spectral vectors to unit length in order to eliminate linear shading effects. While geometric albedo variations are also lost due to this normalization, the method has proven generally useful (*e.g.,* Merényi *et al.,* 1996). The spectral relations are fully retained, and the uniformity gained across spectra of the same material provides for more accurate classification.

The AVIRIS image was classified by both an unsupervised and a supervised Artificial Neural Network (ANN) approach. The particulars of the ANN construction and methodology are given, *e.g.,* in Howell *et al.,* 1994; Merényi *et al.,* 1996, 1997, and Merényi, 1998. The full spectral resolution was utilized. Exclusion of noisy bands following the atmospheric correction resulted in 194 spectral channels. These were input to the classifiers. Preliminarily, 18 spectral classes were identified from the detected clusters. We concentrated on fine discrimination among soil, rock, and mineral classes, and will not interpret the vegetation classes here. The resulting full color thematic map is posted at http://www.lpl.arizona.edu/~erzsebet/erim99.html. Here, in Figure 4, we extracted the classes that are relevant for the detection of locations of alteration.

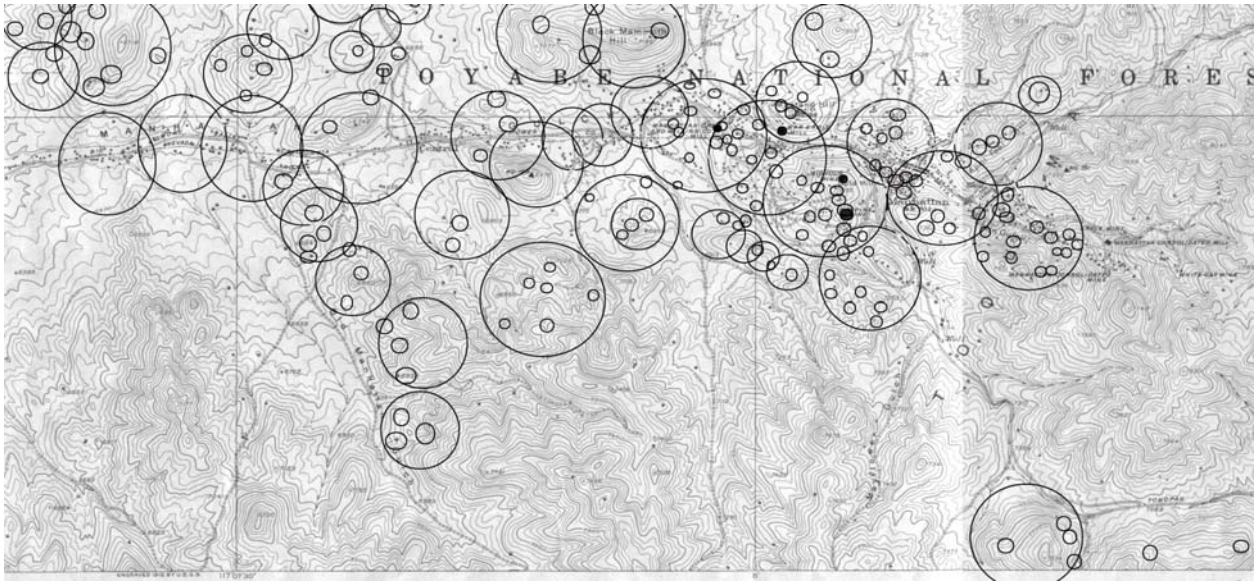

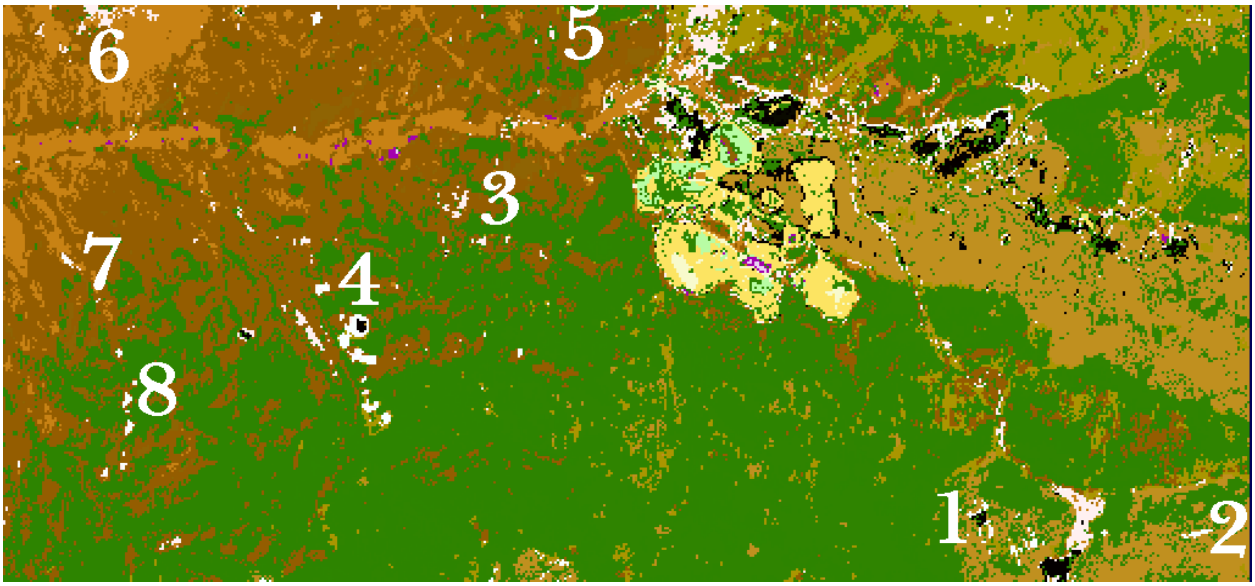

Figure 3 (top). 1:24,000 topographic map of the Manhattan mining area, with some local domes and depressions (large circles) along a NWW trend. A number of localized spots, recommended as targets for detailed exploration, are marked with small circles. The horizontal grid line indicates 38°30" N latitude, and the two vertical grid lines are at 117°7'30" W and 117°5' W, respectively.

Figure 4 (bottom). Extracted classes from a spectral classification map produced from the AVIRIS hyperspectral image. These classes show spectral evidence of iron and clay alteration, as illustrated and discussed in Figure 5. For clarity, in this simplified presentation we highlighted the classes of interest in very light colors and in black (A = black, K, P = white, D = yellow and E = pale yellow). The rest of the 18 spectral classes are shown mostly in dark green and brown colors. (The majority of those are dense vegetation on various soils.) Many occurences, for example those marked by numbers $1-6$, appear at locations very similar to those predicted by doming delineation. The large yellow spots near the center are the Manhattan mines. The black spot at the bottom between #1 and #2 is Jumbo Mine. Alteration is also detected at places (7–8) which are not locations of endogenetic mineralization and therefore are not predicted by dome delineation. A detailed spectral map is visible in color at http://www.lpl.arizona.edu/~erzsebet/erim99.html.

3.0 DISCUSSION OF PRELIMINARY RESULTS

3.1 CORRELATING DOME DELINEATION PREDICTIONS WITH ALTERATION SPECTRA

The Manhattan mining area lies in heavily forested mountainous terrain. Despite the dense vegetation cover, the AVIRIS spectral image yielded useful information. At actual known mine sites, free of interfering vegetation, alteration products were clearly identified at dumps and open pits. At these locations we can readily recognize materials rich in iron oxides or oxihydroxides, and clays. The $\leq$ 100 m areas determined by dome delineation and circled in Figure 3 show a great density in the NW – SE trending fracture zone where most mining sites are concentrated. Figure 5 shows the average signatures of representative spectral classes (A, D, E, K, P, J).

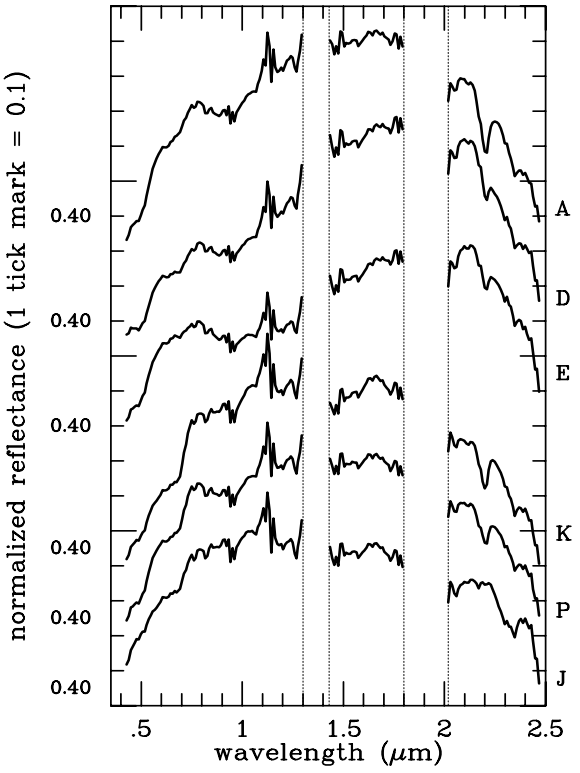

Figure 5. The average spectral signatures of the classes that indicate alteration involving iron oxides or clays. These classes are shown in very light and black colors in Figure 4.

A weak absorption with band minimum at 2.2 and/or 2.3 μm is present in many spectra across the AVIRIS scene. We hypothesize that this is attributable to the black schist parent rock that covers most of the study site. However, the band near 2.2 μm becomes substantially deeper at well defined spots, which may indicate a higher concentration of Al-OH bearing clay minerals such as alunite, kaolinite, jarosite, smectite, or their mixtures. These spots are mapped as classes A, D, E, K, and P (all shown in light color in Figure 4). A band with a minimum at 2.32 μm can indicate chlorite (Mg-OH bearing clay) alteration (class J). Its most conspicuous spatial association is with the gabbro north of the mouth of Manhattan Gulch (#6 in Figure 4). Some of these spectral classes (most clearly A, D, E) show a broad absorption centered at 0.9–0.92 μm, accompanied by a "kink" at 0.5 μm and a cusp near 0.65–0.7 μm. These features typify goethite or jarosite, but jarosite is unlikely because the 2.26 μm narrow absorption band characteristic of jarosite, is not showing. See, *e.g.,* Hunt and Salisbury (1970) and Hunt *et al.,* (1971a,b) for VIS–NIR spectral characteristics of minerals. Similar features seem to be present in class P and perhaps in K, but the spectral signature of the vegetation is mixed in these. We also note that the band minimum near 2.2 μm appears to be at 2.207 μm in these spectra, indicating sericite alteration as its most likely cause (Lyon, 1996, p. 17 and 35). Similar signatures of alteration products were recognized from recent AVIRIS imagery by Crowley and Zimbelman (1996). The noisy spikes near 1.13 μm are residues from atmospheric correction. The gaps between the vertical

dotted lines mark data fallout in the 1.4 and 1.9 μm water bands.

Spectra such as in Figure 5 were mapped at a number of small spots away from major known mines, which also coincide with areas determined by dome delineation. (We are not aware that these locations are functioning mines, and they are not marked as such on the topographic map that we used for dome delineation.) These spots are often small, only a few pixels in extent, partly probably due to the heavy summer vegetation that limited detection to clearings. A good example is provided by the spot NW of Jumbo Mine, #1 in Figure 4, and another, #2, to the East of Jumbo Mine. Further examples include a cluster of spots around #3, some more extended areas near #4, which coincide with major domes, and spectral indications near #5 and #6.

Mineralization on the surface does not necessarily imply the proximity of an ore site. For example, alteration spectra are mapped at outcrops along a road or drainage (#7, #8), but these sites were not detected by dome delineation.

Although we have not yet been able to verify the spectral mapping in the field due to weather conditions at the time of this work, we did collect a small number of rock samples from the vicinity of mines, prior to spectral classification. We will use laboratory spectra of those samples for a limited ground truth. Extensive comparison with standard spectral libraries such as the USGS Speclib (http://speclab.cr.usgs.gov), however, provides reliable identification of alteration signatures.

3.2 UNCERTAINTIES

Because vegetation obscures most of our image away from the main mine sites, many of the ore sites predicted by dome delineation cannot be mapped reliably from our AVIRIS image. In the absence of vegetation dome delineation could still detect possible ore sites where surface mineralization does not occur.

4.0 CONCLUSION AND FUTURE WORK

Spectral remote sensing can be a powerful tool for cost-effective, automated delineation of potential ore sites, detecting alteration minerals on the surface. By combining this with dome delineation, the probability of detecting an ore site and not merely surface mineralization, can be increased significantly.

The study area for this work was defined by the coverage of the AVIRIS image, which included the Manhattan mining site. We have recently acquired new, low-altitude AVIRIS images of another mineralization area, in southern Nevada. Because this region is not covered by vegetation, we will be able to obtain more complete and less ambiguous statistics about the correlation of domes and spectral indication of mineralization. The images are from the first series of AVIRIS' low-altitude flights starting fall, 1998 (http://makalu.jpl.nasa.gov), and are being prepared for distribution at the time of this writing. For our high topography zones the spatial resolution will be about 2–3 m/pixel. Consequently there will be much less spectral mixing than in the present image, and we anticipate finer distinction among a variety of minerals. We will also have a larger area covered by the spectral images.

Although it was not possible to collect field spectra because of snowy conditions at our study site, we plan such measurements next summer along with ground truthing at the new AVIRIS site.

5.0 ACKNOWLEDGEMENTS

EM is partially supported for this work by the Applied Information Systems Research Program of NASA, NAG54001, and by the Pan–American Center for Earth and Environmental Studies (PACES), University of Texas at El Paso. The AVIRIS image was provided by PACES. Technical assistance by Larry Kendall, from the "Science Curriculum To Go" group at LPL, is gratefully acknowledged. NeuralWorks Professional II Plus by NeuralWare, Inc. was used for spectral classification. For image manipulations we used Khoros, ERDAS Imagine, and Adobe Photoshop.

6.0 REFERENCES

Baker, V.R., Finn, V.J., and Komatsu, G., "Morphostructural megageomorphology", *Isr.J. Earth Sci.,* 41, 65–73, 1992.

Crowley, J.K., and Zimbelman, D.R., "Mapping Hydrothermally Altered Rock on Mount Rainier, Washington: Application of AVIRIS Data to Volcanic Hazard Assessments" *In Summaries of the Sixth Annual JPL Airborne Earth Science Workshop*, Pasadena, CA, March 4–8, 1996, Vol. 1: AVIRIS Workshop, Ed. R.O.Green, 1996.

Ferguson, "Geology and ore deposits of the Manhattan District, Nevada", *U.S. Geological Survey Bulletin,* 723, 163, 1924.

B.C. Gao, K.B. Heidebrecht, and A.F.H. Goetz, *Atmosphere Removal Program (ATREM) Version 3.0, User's Guide.* CSES/CIRES, University of Colorado, Boulder, 1997.

E.S. Howell, E. Merényi, L. A. Lebofsky, "Using Neural Networks to Classify Asteroid Spectra", *JGR Planets,* 99 No. E5, 10,847–10,865, 1994.

G.R. Hunt, and J.W. Salisbury, "Visible and Near-Infrared Spectra of Minerals and Rocks: I. Silicate Minerals", *1,* 283–300, , 1970.

G.R. Hunt, J.W. Salisbury, and C.J. Lenhoff, "Visible and Near-Infrared Spectra of Minerals and Rocks: III. Oxides and Hydroxides", *Modern Geology,* 2, 195–205, 1971a.

G.R. Hunt, J.W. Salisbury, and C.J. Lenhoff, "Visible and Near-Infrared Spectra of Minerals and Rocks: IV. Sulphides and Sulphates", *3,* 1–14, , 1971b.

F.J. Kleinhampl and J.I. Ziony, "Mineral Resources of Northern Nye County, Nevada", *Nevada Bureau of Mines and Geology, Bulletin,* 99B, 140–149, 1984.

Lyon, R., "Spectral Properties of Minerals: Applications to the minerals industry", In *Image Processing for Environmental Characterization*, Course Material, ERIM 11th Thematic Conference on Geologic Remote Sensing, Las Vegas, NE, 27–29 February, 1996. pp. 35, 1996.

E. Merényi, Singer, R.B., Miller, J.S., "Mapping of Spectral Variations On the Surface of Mars From High Spectral Resolution Telescopic Images", *ICARUS,* 124, 280–295, 1996.

E. Merényi, E.S. Howell, L.A. Lebofsky, A.S. Rivkin, "Prediction of Water In Asteroids from Spectral Data Shortward of 3 Microns", *ICARUS,* 129, 421–439, 1997.

E. Merényi, "Self-Organizing ANNs for Planetary Surface Composition Research", *European Symposium on Artificial Neural Networks, Bruges, Belgium, 22–24 April, 1998,* , 197–202, 1998.

Sumin–Finn, V., V.R. Baker, A.Z.Dolginov, I.Gabitov, A.Dyachenko, "Large-scale spatial patterns in topography at Alpha Regio, Venus", *Geophys.Res.Letter,* 22, 1901–1904, 1995.